Environmental Science
Processes & Impacts

Precipitation of aqueous transition metals in particulate matter during the dithiothreitol (DTT) oxidative potential assay

Journal:	*Environmental Science: Processes & Impacts*
Manuscript ID	EM-ART-01-2022-000005.R2
Article Type:	Paper

Environmental Significance Statement

Precipitation of aqueous transition metals in particulate matter during the dithiothreitol (DTT) oxidative potential assay

Jayashree Yalamanchili, Christopher J. Hennigan, Brian E. Reed**

The dithiothreitol (DTT) oxidative potential assay is widely used as a measure of particulate matter toxicity. The DTT assay, along with many other chemical measures of oxidative potential, uses a phosphate buffer matrix to maintain the biologically-relevant pH 7.4. In this study, we show that aqueous transition metals present at low concentrations (below 1 μM) undergo rapid precipitation in the DTT assay. Metal precipitation and removal increase with the initial aqueous metal concentration. We observed this phenomenon in experiments with single metals derived from metal salts and in aqueous extracts of urban particulate matter, which contains dozens of metals. This phenomenon has the strong potential to impart bias in the DTT assay, with implications for our understanding of PM toxicity.

Precipitation of aqueous transition metals in particulate matter during the dithiothreitol (DTT) oxidative potential assay

Jayashree Yalamanchili, Christopher J. Hennigan, Brian E. Reed**

Department of Chemical, Biochemical and Environmental Engineering, University of Maryland, Baltimore County, 1000 Hilltop Circle, Baltimore, Maryland 21250, United States.

KEYWORDS: Oxidative potential, DTT, metal precipitation, phosphate buffer, particulate matter.

ABSTRACT: Transition metals in particulate matter (PM) are hypothesized to have enhanced toxicity based on their oxidative potential (OP). The acellular dithiothreitol (DTT) assay is

widely used to measure the OP of PM and its chemical components. In our prior study, we showed that the DTT assay (pH 7.4, 0.1M phosphate buffer, 37 ˚C) provides favorable thermodynamic conditions for precipitation of multiple metals present in PM. This study utilizes multiple techniques to characterize the precipitation of aqueous metals present at low concentrations in the DTT assay. Metal precipitation was identified using laser particle light scattering analysis, direct chemical measurement of aqueous metal removal, and microscopic imaging. Experiments were run with aqueous metals from individual metal salts and a well-characterized urban PM standard (NIST SRM-1648a, Urban Particulate Matter). Our results demonstrated rapid precipitation of metals in the DTT assay. Metal precipitation was independent of DTT but dependent on metal concentration. Metal removal in the chemically complex urban PM samples exceeded the thermodynamic predictions and removal seen in single metal salt experiments, suggesting co-precipitation and/or adsorption may have occurred. These results have broad implications for other acellular assays that study PM metals using phosphate buffer, and subsequently, the PM toxicity inferred from these OP assays.

Introduction

Particulate matter (PM) exposure causes acute and chronic effects on human health, including premature mortality.[1, 2] Many of the detrimental outcomes associated with PM exposure may result from oxidative stress, whereby reactive oxygen species (ROS) are catalytically formed due to reactions with components present in PM.[3-9] Evidence suggests that transition metals are among the most toxic constituents of atmospheric particles[10, 11] even though they typically constitute a tiny fraction of PM mass.[12] Metals are redox-active and can catalyze ROS formation[13-15], providing a plausible explanation for their enhanced toxicity.[13, 16]

At present, there is not a gold-standard method for the measurement of oxidative stress or ROS generation in air pollution exposure assessment.[11, 17, 18] Experimental methods to measure PM toxicity can be broadly classified into three categories: 1) direct measurements of human physiology and biomarkers; 2) animal model studies, and 3) *in vitro* assays (which include both cellular and acellular techniques). Due to the immense savings of time and cost over biological methods[19, 20], acellular *in vitro* assays have seen widespread adoption in atmospheric studies globally.[21-30] The dithiothreitol (DTT) assay is widely used,[13, 24, 27, 31-34] due to its linear relationship demonstrated with the cellular heme oxygenase-1 assay.[35] To increase its biological relevance, the DTT assay is conducted at 37 ˚C and pH 7.4, the latter maintained using a

phosphate buffer. However, prior work from our group found that precipitation of multiple metals (Fe(II), Fe(III), Mn, and Cu) occurred under the DTT assay conditions.[36] Further, the complexation of metal cations with phosphate can affect metal-ion-dependent reactions[37], including ROS generation. The complexation of transition metals with a phosphate buffer has been identified as an important phenomenon influencing DTT depletion during the assay.[38]

Metal precipitation in a phosphate buffer matrix is unsurprising. For example, Fe(III) addition is a well-known strategy for removing phosphate (PO_4) during wastewater treatment.[39-41] In our prior study, the thermodynamic predictions were validated at high aqueous metal concentrations with experiments during which visible precipitates formed.[36] However, metal precipitation has not been demonstrated at lower metal concentrations (< 50 μM) representative of PM samples (i.e., aqueous filter extracts). The reactivity of metals and PM, including the generation of ROS, vary due to their phase (aqueous vs. solid) and oxidation state.[11,42-45] Based on the solubility of metals in the PM extraction solvent, there could be a significant effect on oxidative potential (OP) measurements that utilize phosphate-based assays.[46-48] Both soluble and insoluble fractions of metals in PM can be correlated to ROS activity, though they induce different responses in OP.[42,43] Because the acellular assays are used as a proxy for PM toxicity[35], it is necessary to

understand the phenomena occurring from the interaction of metals with the phosphate buffer. The objective of this study is to characterize the precipitation of aqueous metals in the DTT assay. We use urban PM samples containing dozens of metals present in aqueous extracts at low concentrations (0.1 – 20 μM). Precipitation when aqueous metals from PM extracts and metal-salts are added to the DTT assay is detected using a combination of approaches. Our analysis is focused on Fe (Fe(II) and Fe(III)) because of its high concentration in PM[49, 50], and Cu(II) and Mn(II) due to their high reactivity in the DTT assay.[13, 51, 52] Precipitate formation and metal removal in the chemically complex PM extracts are compared to experiments conducted with metal salts to elucidate interactions and effects of multiple species in the DTT assay matrix.

Methods

Chemicals

The following chemicals were used: ferric chloride hexahydrate (99.9%, Fisher Scientific), copper(II) sulfate (Reagent grade, Alfa Aesar), manganese(II) chloride tetrahydrate (99%, ACROS organics), iron(II) chloride tetrahydrate (99%, ACROS organics), potassium phosphate dibasic (98%, Fisher BioReagents), potassium phosphate monobasic (99%, Fisher BioReagents), 1,4-dithiothreitol (DTT, 99%, ACROS organics), and nitric acid (Reagent grade, Alfa Aesar).

All metal stock solutions were prepared in 2% nitric acid, with aqueous metal concentrations measured using ICP-MS (PerkinElmer, NexION 300D). The concentration of the Fe(II) stock solution was regularly measured by colorimetry to ensure there was no oxidation of Fe(II). The DTT solution was prepared fresh in a 0.1 M phosphate buffer on the day of each experiment.

NIST urban PM- SRM-1648a extract

National Institute of Standards and Technology SRM-1648a (Urban Particulate Matter) is a well-characterized reference material collected from the urban atmosphere of St. Louis, MO.[53] SRM-1648a has been widely used because of its certified composition and the connection it enables across various studies that are not possible with variable PM composition.[54-62] SRM-1648a contains dozens of metals whose concentrations are given in Table S1. An aqueous stock solution of the urban PM extract was prepared by adding 200 mg of SRM-1648a to 200 mL of 0.1 N HNO_3, stirred at 200 rpm for 24 hours, and vacuum filtered (Tissue Quartz 2500qat-up filter).[63-66] Aqueous metal concentrations in the SRM-1648a PM extract are given in Table 1. The extract was stored in a high-density polyethylene (HDPE) vial for the SRM-1648a extract experiments. Metal concentrations in the extract were measured using ICP-MS, while Fe, Mn, and Cu were also measured using colorimetric analysis (see discussion below). There was

excellent agreement in the Fe, Mn, and Cu measurements using both methods (Table S2 and S3). ICP-MS analysis of metals suffers from matrix effects when high salt concentrations are present, as is the case in the DTT assay (0.1 M PO_4 made from KH_2PO_4 and K_2HPO_4, ionic strength = 0.29 M)[67, 68] (Figure S1, Table S3). Therefore, removal of Fe, Mn, and Cu was measured using colorimetric analysis in most experiments.

Precipitation in DTT Assays

Following the DTT assay procedure of Cho et al. [69], the aqueous sample (either SRM-1648a extract or metal salt solution) was incubated with 100 μM DTT in a 0.1 M phosphate buffer at a pH of 7.4 and a temperature of 37 ± 3 ˚C for 30 minutes. For metal salt experiments, metals were added from their salt solution individually or as a combination of Fe, Mn, and Cu. The particle number concentration was continuously measured using laser particle light scattering (Mastersizer 3000, Malvern Panalytical).[70-76] Monodispersed polystyrene latex (PSL) microspheres (0.5 μm) with 2.5 weight% dispersion in water were used to calibrate the instrument, laser obscuration (the parameter measured by the instrument) and particle number concentration (r^2 of 0.99, Figure S2). The baseline was measured in each experiment for 10 minutes prior to sample addition to the DTT assay. Immediately at the end of the assay, an

aliquot from the incubation step was filtered (0.45 μm PTFE syringe filter, Restek Corporation), and the aqueous metal concentrations were measured using colorimetric analysis due to the interferences present in the ICP-MS measurements as described above. Therefore, total Fe, Fe(II) (Fe(III) was calculated by the difference), Cu(II), and Mn(II) were measured using colorimetric methods (HACH DR/890)[77-80]. The accuracy of the colorimetric analyses was verified via ICP-MS in DI water and the phosphate buffer matrix (Figure S1, Table S3). The method detection limit for Fe, Mn, and Cu is 0.5 μM in DI water; 0.5, 1.0, and 1.4 μM, respectively, in 0.1 M phosphate buffer matrix. Metal removal was calculated based on the initial aqueous metal concentration and the final measured concentration in the filtered extract by colorimetric analysis. Note that the calculations of metal removal are based on the colorimetric measurements while Table 1 has the metal concentrations in the PM extract measured by ICP-MS, and hence there is a minor difference in the values (Table S2). After 30 minutes of the DTT assay, solutions were filtered (Tissuequartz 2500 qat-up filter) and collected for particle imaging. The filtered solids were vacuum dried and twice washed with 50% ethanol/H_2O to remove residual buffer. Any precipitates formed during the DTT assay were characterized using transmission electron microscopy (TEM) and scanning electron microscopy (SEM) imaging coupled with energy dispersive spectroscopy (EDS). TEM was used to determine particle size, while SEM-EDS

determined the morphology, and the various elements present in the filtered precipitates. TEM analyses were carried out using an FEI Morgagni 268 100 kV TEM equipped with a Gatan Orius CCD camera. SEM analyses utilized an FEI Nova NanoSEM 450 SEM with Energy-dispersive X-ray spectroscopy. The TEM samples (10 μl) were pipetted onto the grid, dried in the atmosphere by wicking the solution off the carbon-coated and formvar-coated copper sample grid, while the SEM samples were dried on a carbon tape substrate, also in ambient air. All the above procedures and analyses were run with and without DTT present to characterize any effects on metal precipitate formation for SRM-1648a extract samples at low concentrations. All experiments were run in triplicate unless otherwise noted.

Results and Discussion

Metal precipitation of NIST urban PM (SRM-1648a) in the DTT assay

For the precipitation experiments, SRM-1648a extract was added to the DTT assay at three concentration levels (Table 1), which were selected according to the range of Fe concentrations measured in ten urban areas across the US using accepted PM filter sampling and extraction protocols[36, 49, 50]. The concentrations of the remaining elements were calculated based on the dilution factor (DF) and the elements' concentration in the SRM-1648a extract. Note that the Cu concentration for samples 1, 2, and 3 and Mn concentration for samples 1 and 2 were below the DL for the colorimetric analysis. To maintain the relevance of Mn and Cu concentrations to that in PM filter extracts (0.058 μM Mn and 0.06 μM Cu) [36, 49, 50], increasing the SRM-1648a sample

concentrations above DL for Mn and Cu was not preferred. Also presented in Table 1 are metal solubilities and saturation indexes (SI) determined by MINEQL[36, 81] under the DTT assay conditions (0.1 M $TOTPO_4$, T = 37°C, pH =7.4 and ionic strength = 0.22 M). The modeling approach used is based on our previous work[36] (thermodynamic data are presented in Table S7, and detailed results from thermodynamic modeling are presented in Tables S8 and S9). In Table 1, metals with an asterisk (Al, Ca, Fe, Mn, and Pb) indicate species that can theoretically precipitate (i.e., those with a positive saturation index (SI)).

We recognize that it is unlikely that equilibrium was reached given the short reaction time (< 1 hr) and the use of equilibrium modeling serves only as a framework for understanding what may be occurring in PO_4-based assays. In addition, we acknowledge the uncertainty that arises with equilibrium modeling due to: (1) the inherent difference in reported equilibrium constants, (2) assuming equilibrium conditions for systems that may not be at equilibrium, and (3) applying constants determined under specific experimental conditions (metal concentration, temperature and ionic strength) to systems having different conditions. To access the uncertainty in values of K_{s0}, we conducted a sensitivity analysis on K_{s0} ($\log K_{s0} \pm 2$) on the saturation index for the precipitates that we believe formed (Figure S3). For all values of K_{s0} the SI for Ca, Fe(III), Mn, and Pb was always positive while for Al the SI was only negative at $\log K_{s0}$ -2, indicating that precipitation was thermodynamically possible over a wide range of K_{s0}'s.

Table 1. The experimental concentrations, solubilities, and saturation indices for the major elements in the SRM-1648a extract (average ± SD, n=3 replicates). Metals with an asterisk

indicate that precipitate formation is thermodynamically possible under DTT assay conditions (0.1 M $TOTPO_4$, T = 37°C, pH =7.4 and ionic strength = 0.22 M). Three dilutions of the SRM-1648a extract were used in particle number and direct measurement experiments.

Metal	SRM-1648a acid extract, μM	Concentrations, μM (Saturation Index[1])			Metal solubility[2], μM	Precipitate form
		Sample 1 DF = 50.5	Sample 2 DF = 16.1	Sample 3 DF =5.6		
Al*	114.0 ± 3.8	2.3 (0.7)	7.1 (1.2)	20.3 (1.6)	4.7×10^{-1}	γ-$Al(OH)_3$
Ca*	490.0 ± 9.7	9.8 (0.9)	30.6 (3.3)	87.3 (5.6)	6.6	$Ca_{10}(PO_4)_6(OH)_2$
Co	1.3 ± 0.02	0.03 (-5.5)	0.1 (-4.0)	0.2 (-3.1)	2.1	$Co_3(PO_4)_2$
Cr	2.5 ± 0.05	0.1 (-0.9)	0.2 (-0.6)	0.5 (-0.2)	2.7×10^{-3}	$Cr(OH)_3$
Cu	4.5 ± 0.1	0.1 (-5.0)	0.3 (-3.5)	0.8 (-2.2)	4.5	$Cu_3(PO_4)_2$
Fe (total)	106.0 ± 7.9	2.1	6.6	18.9		
Fe(III)*	102.0 ± 7.6	2.0 (3.6)	6.4 (4.1)	18.1 (4.6)	5.1×10^{-4}	$FePO_4.2H_2O$
Fe(II)	4.0± 0.3	0.1 (-4.4)	0.3 (-2.9)	0.7 (-1.8)	2.9	$Fe_3(PO_4)_2$
Mg	159.0 ± 8.6	3.2 (-2.6)	10.0 (-2.1)	28.4 (-1.6)	1.2×10^{3}	$MgHPO_4{:}3H_2O$

Mn*	6.7 ± 0.2	0.1 (2.6)	0.4 (3.2)	1.2 (3.37)	2.6 x10^{-4}	$MnHPO_4$
Ni	1.7 ± 0.03	0.03 (-8.7)	0.1 (-7.2)	0.3 (-5.7)	24.2	$Ni_3(PO4)_2$
Pb*	22.3 ± 0.7	0.4 (9.2)	1.4 (10.8)	4.0 (12.2)	3.5 x10^{-4}	$Pb_3(PO_4)_2$
V	1.9 ± 0.1	0.04 (-11.9)	0.1 (-11.5)	0.3 (-11.0)	3.2x10^{10}	$V(OH)_3$
Zn	37.1 ± 2.0	0.7 (-1.5)	2.3 (0.1)	6.6 (1.5)	2.2	$Zn_3(PO_4)_2$

[1]Saturation index (SI) = log(ion activity product/solubility product). A positive value of SI indicates that precipitation is thermodynamically possible. [2]Summation of all aqueous metal species.

(a) (b)

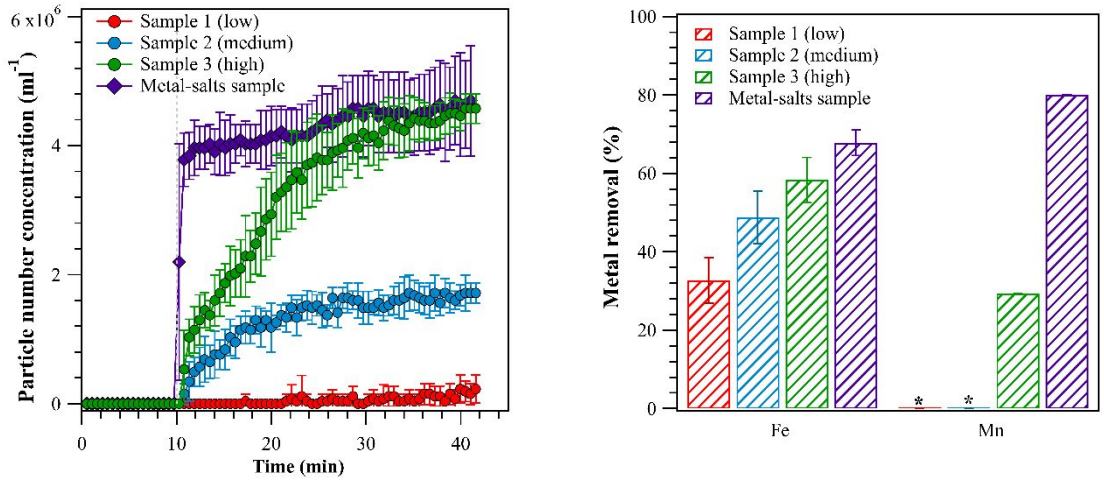

Figure 1. (a) Evolution of the particle number concentration when aqueous samples were added to the DTT assay. Sample addition occurred after 10 minutes of baseline measurements (vertical dotted line). Table 1 gives the composition and metal concentrations

for SRM-1648a samples (samples 1, 2, and 3). The metal-salts sample contained a mixture with 50 μM Fe(III), 5 μM Fe(II), 5 μM Mn(II), and 5 μM Cu(II). **(b)** Average Fe and Mn removal at time = 30 minutes in the DTT assay. The asterisks in (b) represent initial Mn concentrations below the DL so that metal removal could not be measured.

The particle number concentration was measured continuously for the three SRM-1648a samples during incubation (30 minutes, 1800 rpm) in the DTT assay (Figure 1a). After 30 minutes, samples were taken, filtered (0.45 μm), and analyzed for aqueous Fe and Mn concentrations (Figure 1b). Note that the initial Mn concentration in samples 1 and 2 was less than the colorimetric analysis DL (1 μM). The particle number concentration-response for samples 2 and 3 clearly indicates the rapid formation of precipitates, while the response for sample 1 was slightly above the 0-10 minutes baseline period (i.e., before the SRM-1648a extract was added). The precipitate formation was confirmed based on aqueous metal content at the end of the incubation period (Figure 1b). Total Fe removal via precipitation for samples 1, 2, and 3 was 33 ± 6%, 49 ± 7%, and 58 ± 6%, respectively. The extent of Fe removal was independent of the mixing speed during the incubation (Figure S4). There was significant Fe precipitation for sample 1, which had a particle number concentration only slightly above the

baseline. Although the particle number concentration was low for sample 1, precipitation in this sample was further confirmed through SEM imaging (detailed discussion below). The initial Fe(II) concentrations in samples 1 and 2 were below the colorimetric analysis DL (0.5 μM). The initial Fe(II) concentration of sample 3 was 0.8 μM, and after 30 minutes of incubation, the Fe(II) concentration was below the DL (0.5 μM), indicating that Fe(II) precipitated as $Fe_3(PO_4)_2$(s) or was oxidized to Fe(III) with subsequent precipitation as $Fe(PO_4)$(s). Fe(II) oxidization to Fe(III) was also observed in our prior work[36].

The initial Mn concentrations in samples 1 and 2 were below the colorimetric analysis DL (1.0 μM), while for sample 3, it was 1.4 μM (note that the ICP initial Mn was 1.2 μM, Table S2). After the incubation period, the total aqueous Mn was below the 1.0 μM DL resulting in an Mn removal of at least 29% for sample 3. Mn can exist as Mn(II), Mn(III), and Mn(IV)[38], and these forms of Mn can precipitate as $MnHPO_4$, MnO(OH), and MnO_2 (Table S7) and undergo oxidation reactions (Mn(II)→Mn(III); Mn(III)→Mn(IV)). The Mn colorimetric analysis measures the total Mn. Thus, the Mn from the SRM-1648a particulate matter was either directly precipitated or oxidized with subsequent precipitation. In our earlier work where we used an Mn(II) salt ($Mn(Cl)_2$) as the source of Mn, we observed that Mn(II) was oxidized to Mn(IV) followed by Mn(IV) precipitation as MnO_2 [36].

Precipitation experiments were also conducted using salts ($Fe(III)Cl_3$, $Fe(II)Cl_2$, $Mn(II)Cl_2$, $Cu(II)SO_4$) as the source of metals added to the DTT assay. The sample containing mixed metal-

salts (50 μM Fe(III), 5 Fe(II), 5 μM Mn(II), and 5 μM Cu(II)) precipitated immediately upon addition to the DTT assay and showed a particle number concentration at the end of the incubation period that was similar to SRM-1648a sample 3. For sample 3, the initial Fe, Mn, and Cu concentrations were much lower than those used in the metal salt experiments. The similar particle formation suggests that precipitation of other metals present in the SRM-1648a extract occurred (e.g., Al, Ca, Pb can form $Al(OH)_3$, $Ca_{10}(PO_4)_6(OH)_2$, $Pb_3(PO_4)_2$, respectively, details in SI). The faster formation of particles in the mixed metal-salt sample could be due to the ease of Fe(III) precipitation. In our earlier work, we observed that the rate of precipitation increased with the initial Fe concentration[36]. At the end of the metal-salts incubation period Fe(III), Fe(II), and Mn(II) concentrations were 17.8 ± 1.8 μM, 0.2 ± 0.2 μM, and 0.6 ± 0.1 μM, respectively. Total Fe removal in the mixed metal-salts sample was 68 ± 3%, similar to 58 ± 6% observed for the SRM-1648a sample 3. Fe(II) was either oxidized to Fe(III) or was directly precipitated as $Fe_3(PO_4)_2(s)$. For Mn, the aqueous concentrations at the end of the incubation period were less than the DL (1 μM Mn), resulting in removal of at least 80.0 % for metal-salt experiments compared to 29% for SRM-1648a sample 3. We note that both are lower bounds as the Mn removal may have been higher in each sample.

Based on the above results, it is clear that metal precipitation (and possibly oxidation) occurs rapidly during acellular assays that use a matrix with phosphate buffer. The extent of precipitation appears to depend on the initial concentration of metals present. We hypothesize that increasing the concentration of metals initially present (especially the easily precipitated Fe(III)) increases nucleation as well as the potential for co-precipitation and adsorption.

Effect of DTT on metal precipitation

To characterize the effects of DTT on metal precipitation, particle number concentrations (Figure 2a) and aqueous metal concentrations (Figure 2b) were measured with and without DTT addition. There was no statistically significant difference in the presence and absence of DTT ($p > 0.05$ for samples 1,2 and 3).

(a) (b)

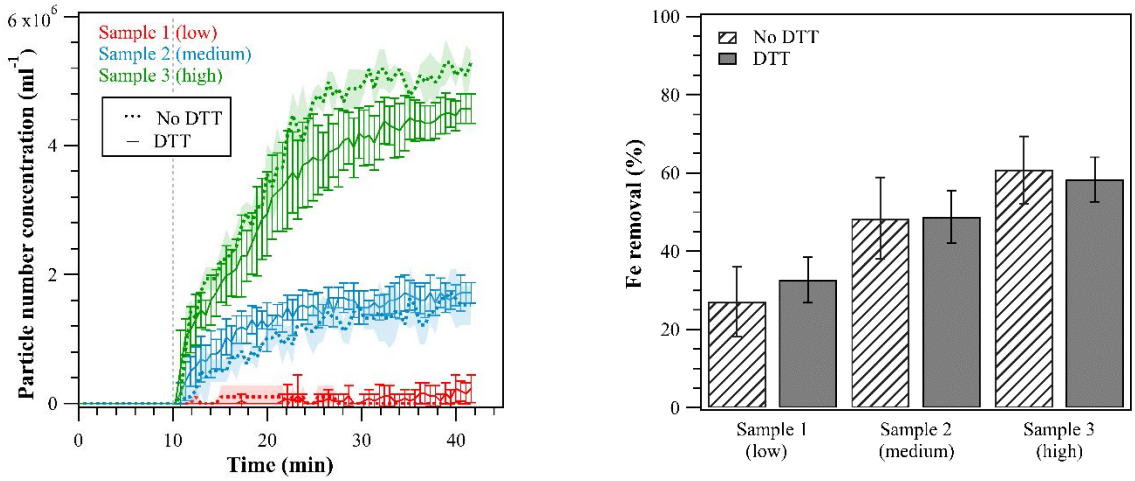

Figure 2. **(a)** Average evolution of the particle number concentration of SRM-1648a extract samples in the presence and absence of DTT, observed after its addition to a 0.1M phosphate buffer at pH 7.4 and 37 ± 3 ˚C at a time of t= 10 minutes. **(b)** Average Fe removal in filtered samples for SRM-1648a extract in the presence and absence of DTT at pH 7.4 and 37 ± 3 ˚C.

Fe removal (Figure 2b) measured at the end of the incubation period showed no statistically significant difference for samples 1, 2, and 3 ($p > 0.05$). Although chemical analysis could not confirm the effect of DTT on Mn and Cu removal, the particle number concentrations and Fe removal results strongly suggest that precipitation is not significantly affected by the presence of DTT. Thus, MINEQL modeling results can inform the extent of metal precipitation at low metal concentrations (Table S5), and Cu removal can be examined in the absence of DTT. These observations agree with our previous work in which we also found no effect of DTT on metal precipitation at higher metal concentrations[36].

Metal precipitate identification

TEM and SEM were used to confirm the presence of solids, obtain morphological details and identify elements present in the precipitates (Figures 3, S5, and S6).

(a)

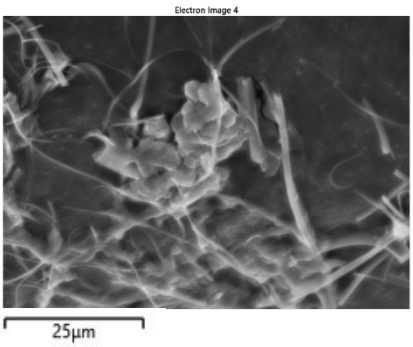

(b)

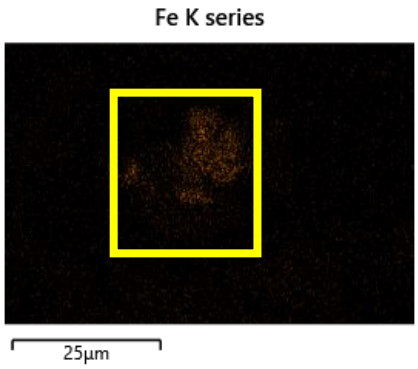

(c) (d)

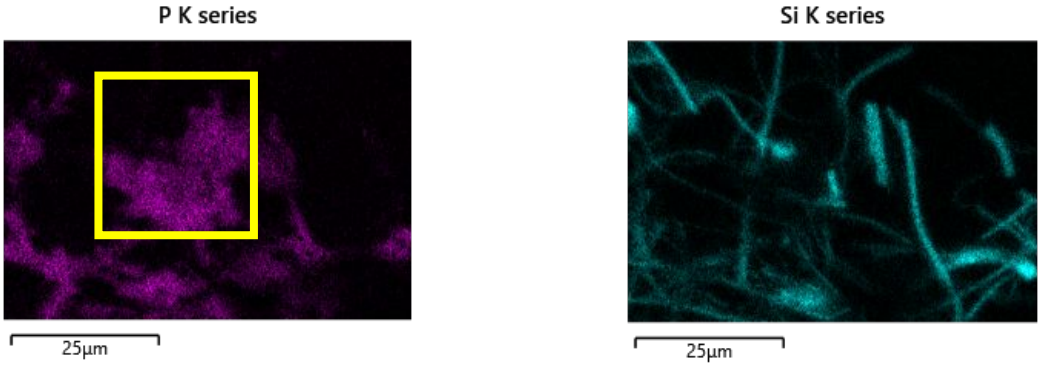

Figure 3. Scanning electron microscopy images of SRM-1648a extract sample 1 filtered after 30 minutes in the DTT assay matrix with 0.1M phosphate buffer with a pH of 7.4 and a temperature of 37 ± 3 ˚C. Figure 3**(a)** shows a solid cluster. The elemental map of the solid cluster indicates the main elements of interest:**(b)** Fe, **(c)** P in SRM-1684a sample 1. Figure 3**(d)** shows the elemental map of the Si present in the filter substrate.

Samples for microscopic analysis were prepared by filtering the DTT assay solution after the 30 minutes incubation and washing (twice) the filtered residue with 50% ethanol to remove phosphate. TEM results confirm the presence of the solid particles in the 0.2 μm range (Figure S5) in the absence and presence of DTT.

SEM images confirm the presence of the solids containing Fe in the visible clusters (Figure 3b). Precipitation in SRM-1648a sample 1 (the lowest concentration) is confirmed by SEM-EDS

despite low particle number concentrations measured for this sample (Figure 1a). Similar results were observed in the absence of DTT and for SRM-1648a samples 2 and 3 (Figure S6). It is important to note that the cluster size shown in Figure 3a was likely affected by the air-drying process required for SEM analysis and may not represent the size of the precipitates formed during the DTT assay. The P identified in Figure 3c is associated with metal precipitates, assuming that the ethanol wash performed in duplicate effectively removed aqueous PO_4 prior to the drying step. The Si detected by SEM (Figure 3d) is from the quartz filter. SEM images for samples 2 and 3 are in Figure S6 and similarly show precipitates as a cluster in the presence and absence of DTT.

In addition to Fe and P, the SEM-EDS identified a number of additional metals in the filtered precipitates, including Cu, Pb, Ca, Al, Mg, V, Ti, and Zn. All of the detected species are present in the SRM-1648a extract. It is interesting to note that Cu, V, and Zn precipitation was not predicted thermodynamically because these metals' concentrations in the SRM-1648a samples are below their solubilities (Table 1). Their detection in the precipitated particles indicates that co-precipitation or possible adsorption by other precipitates may have occurred. Based on the variability in PM composition and concentration, it is likely that both precipitation and the extent of aqueous metal removal will exhibit variability for different samples. This suggests that predictions of this phenomenon cannot occur without *a priori* knowledge of sample characteristics. However, our observations of precipitation and metal removal in the simplest

sample compositions (single metal salts) performed at low concentrations suggest that this phenomenon is pervasive during the DTT assay, potentially leading to an artifact in the oxidative potential measurements.

Fate of Fe(II), Fe(III), Cu(II), and Mn(II) in the DTT assay

Amongst the many metals present in ambient PM, the precipitation/oxidation of Fe(II), Fe(III), Mn(II), and Cu(II) in the DTT assay were investigated individually because of their elevated concentrations (Fe) or high reactivity in the DTT assay (Cu and Mn)[13, 51, 52, 82-84]. Metal concentrations between 5 μM - 100 μM were examined. In our previous work, at higher Cu concentrations, DTT had no effect on Cu precipitation[36]. Therefore, the measurements of Cu removal occurred without DTT addition because DTT interferes with the colorimetric analysis.

(a) (b)

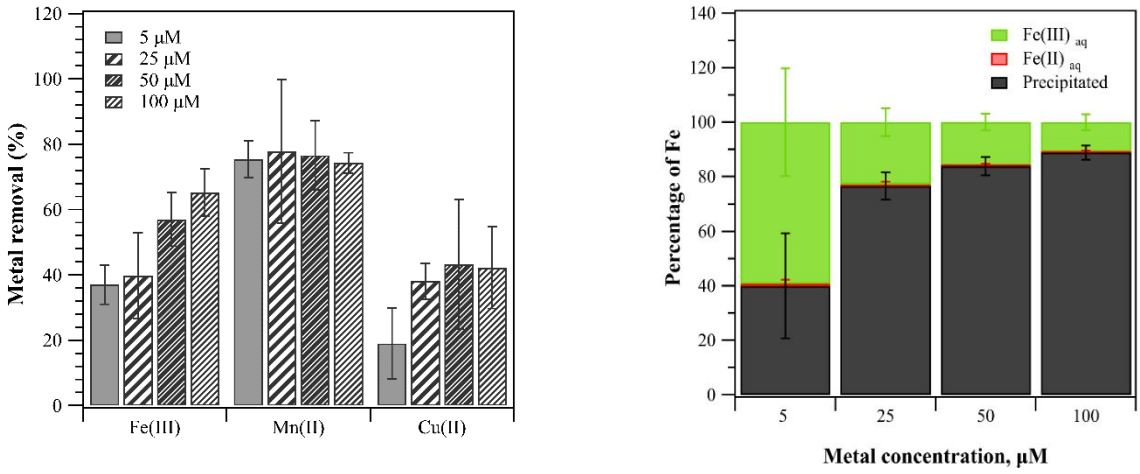

Figure 4. (a) Metal removal measured for each of the individual metal-salts experiments and **(b)** the fate of Fe(II) at time = 30 minutes in the DTT assay (0.1M phosphate buffer, pH 7.4 and 37 ˚C) as a function of the initial Fe(II) concentration.

Fe(III) precipitation (Figure 4a) generally increased with increasing initial Fe concentration. For Fe(II), there was significant oxidation to Fe(III) (Figure 4b) at the end of the incubation period; Fe(III) was present for all experiments, and the aqueous Fe(II) ranged from only 0.3 to 0.7% of the total Fe(II) initially added. Fe(II) and the formed Fe(III) precipitated as $Fe(II)_3(PO_4)_2(s)$ or $Fe(III)PO_4(s)$. Fe(II) and Fe(III) particle number concentration results (Figures S7a and S7b) were consistent with the data in Figures 4a and 4b. The results from Fe(III) metal-salts and SRM-1648a experiments for similar initial Fe(III) concentrations were consistent: Fe removal for 25 μM Fe(III) and SRM-1648a sample 3 (20.7 μM Fe) were 40 ± 13% and 58 ± 6%, respectively. Similarly, Fe removal for 5 μM Fe(III) and SRM-1648a sample 2 (7.3 μM Fe) were 37 ± 6% and 49 ± 7%, respectively. The slightly higher removal for the SRM-1648a samples could be due to the formation of other precipitates (e.g., $Al(OH)_{3(s)}$), which would increase removal through enhanced nucleation, co-precipitation, and adsorption.

Mn(II) removal (Figure 4a) was independent of its initial concentration ($p > 0.05$). Particle number concentrations increased with the increasing initial Mn concentration (Figure S7c), though the metal removal was not dependent on the initial concentration. Similar to Mn, Cu removal was also not dependent on the initial Cu concentration.

Conclusions

Our findings demonstrate that aqueous metals undergo rapid phase change in the DTT assay due to precipitation, co-precipitation, adsorption, and/or enhanced nucleation of metals. Multiple analyses confirmed the precipitation of metals in SRM-1648a extract and metal-salts in the DTT assay (37 ˚C, 7.4 pH, 0.1 M phosphate buffer). Precipitation occurred at low concentrations of metals, similar to that in ambient PM filter extracts, and scales that are not visible to the naked eye. There was increased metal removal in the SRM-1648a extract samples compared to metal salts, likely due to co-precipitation, adsorption, and/or enhanced nucleation. Metal removal was dependent on the initial metal concentration and the sample composition, suggesting a complex phenomenon that may affect assay results differently depending on sample characteristics. Therefore, the extent of metal precipitation in the DTT assay is likely to vary between samples collected at different times and in different environments. The metals that were shown to precipitate or co-precipitate (Fe, Mn, Al, Ca, Pb, Mg, Zn, Cu, V) may affect DTT assay results[38, 85-87] as both soluble and insoluble fractions of metals in PM can affect ROS production differently[42, 43, 46, 47].

The DTT assay, which is widely used to quantify oxidative potential in PM studies, is likely affected by the phenomena reported in this study, as we observed dramatic changes in the

aqueous concentrations of species that are highly redox active. Metal precipitation in the DTT assay may contribute to the weak relationship observed between the DTT assay and cellular assays such as macrophage ROS assay and H2DCFDA[88-90]. The effects of metal precipitation on the DTT assay for are beyond the scope of this study but are the subject of ongoing work in our lab. These results likely have implications for other phosphate-based acellular assays, such as ascorbic acid (AA), 2′,7′-dichlorofluorescein (DCFH), and glutathione (GSH)[17]. Thus, understanding the fate of soluble metals in those assays is a pressing research need to fully assess their application for particle toxicity measurements.

The proposed research also has broad implications beyond PM toxicity. Phosphate, added as $Na_xH_yPO_4$ or $K_xH_yPO_4$ (with x and y summing to 3), is a common ingredient in many surrogate biological fluids, including Simulated Body Fluid, Updated Simulated Body Fluid, Simulated Synovial Fluid, Simulated Colonic Fluid 1, Simulated Saliva, Simulated Semen Solution 1, and Simulated Sweat[91]. The various forms of Simulated Lung Fluid (SLF) all contain sodium phosphate buffer[91]. Synthetic biological fluids are used in a wide array of biomedical research, including drug delivery and release. Many of these synthetic biological fluids have pH = 7 – 7.5, which suggests transition metal precipitation likely occurs in these matrices. Aqueous metal removal is possible,

even when metals are present below their saturation concentration, due to co-precipitation and/or adsorption. Therefore, the phenomenon identified in this work may introduce unwanted artifacts and biases in other systems that contain phosphate.

ASSOCIATED CONTENT

Supporting Information.

The following files are available free of charge.

Summary of the laser particle light scattering analysis and colorimetric analysis, along with the method limitation and DL; effect of mixing speed on metal removal; list of various elements in SRM-1648a; modeling conditions and solubilities of different solids obtained from MINEQL; TEM images for all SRM-1648a samples; SEM images for SRM-1648a samples 2 and 3; SEM-EDS weight distribution range for SRM-1648a samples 1 and 3. (PDF)

AUTHOR INFORMATION

Corresponding Author

*C.J. Hennigan. Email: hennigan@umbc.edu; phone: (410) 455-3515. *B.E. Reed. Email: reedb@umbc.edu; phone: (410) 455-8154.

Author Contributions

The manuscript was written through the contributions of all authors. All authors have given approval to the final version of the manuscript.

Funding Sources

This work was funded by the National Science Foundation through award #1802474.

Notes

The authors declare no competing financial interest.

ACKNOWLEDGMENT

We acknowledge Joshua Wilhide and Maggie LaCourse, UMBC- Molecular characterization and analysis complex for assistance with the ICP-MS analysis, Tagide deCarvalho, Director, UMBC- Keith R. Porter imaging facility for assistance with TEM and SEM-EDS analysis.

REFERENCES

1. J. O. Anderson, J. G. Thundiyil and A. Stolbach, Clearing the Air: A Review of the Effects of Particulate Matter Air Pollution on Human Health, *Journal of Medical Toxicology*, 2012, **8**, 166-175.

2. S. S. Lim, T. Vos, A. D. Flaxman, G. Danaei, K. Shibuya, H. Adair-Rohani, M. A. Almazroa, M. Amann, H. R. Anderson, K. G. Andrews, M. Aryee, C. Atkinson, L. J. Bacchus, A. N. Bahalim, K. Balakrishnan, J. Balmes, S. Barker-Collo, A. Baxter, M. L. Bell, J. D. Blore, F. Blyth, C. Bonner, G. Borges, R. Bourne, M. Boussinesq, M. Brauer, P. Brooks, N. G. Bruce, B. Brunekreef, C. Bryan-Hancock, C. Bucello, R. Buchbinder, F. Bull, R. T. Burnett, T. E. Byers, B. Calabria, J. Carapetis, E. Carnahan, Z. Chafe, F. Charlson, H. Chen, J. S. Chen, A. T.-A. Cheng, J. C. Child, A. Cohen, K. E. Colson, B. C. Cowie, S. Darby, S. Darling, A. Davis, L. Degenhardt, F. Dentener, D. C. Des Jarlais, K. Devries, M. Dherani, E. L. Ding, E. R. Dorsey, T. Driscoll, K. Edmond, S. E. Ali, R. E. Engell, P. J. Erwin, S. Fahimi, G. Falder, F. Farzadfar, A. Ferrari, M. M. Finucane, S. Flaxman, F. G. R. Fowkes, G. Freedman, M. K. Freeman, E. Gakidou, S. Ghosh, E. Giovannucci, G. Gmel, K. Graham, R. Grainger, B. Grant, D. Gunnell, H. R. Gutierrez, W. Hall, H. W. Hoek, A. Hogan, H. D. Hosgood, D. Hoy, H. Hu, B. J. Hubbell, S. J. Hutchings, S. E. Ibeanusi, G. L. Jacklyn, R. Jasrasaria, J. B. Jonas, H. Kan, J. A. Kanis, N. Kassebaum, N. Kawakami, Y.-H. Khang, S. Khatibzadeh, J.-P. Khoo, C. Kok, F. Laden, R. Lalloo, Q. Lan, T. Lathlean, J. L. Leasher, J. Leigh, Y. Li, J. K. Lin, S. E. Lipshultz, S. London, R. Lozano, Y. Lu, J. Mak, R. Malekzadeh, L. Mallinger, W. Marcenes, L. March, R. Marks, R. Martin, P. McGale, J. McGrath, S. Mehta, Z. A. Memish, G. A. Mensah, T. R. Merriman, R. Micha, C. Michaud, V. Mishra, K. M. Hanafiah, A. A. Mokdad, L. Morawska, D. Mozaffarian, T. Murphy, M. Naghavi, B. Neal, P. K. Nelson, J. M. Nolla, R. Norman, C. Olives, S. B. Omer, J. Orchard, R. Osborne, B. Ostro, A. Page, K. D. Pandey, C. D. Parry, E. Passmore, J. Patra, N. Pearce, P. M. Pelizzari, M. Petzold, M. R. Phillips, D. Pope, C. A. Pope, J. Powles, M. Rao, H. Razavi, E. A. Rehfuess, J. T. Rehm, B. Ritz, F. P. Rivara, T. Roberts, C. Robinson, J. A. Rodriguez-Portales, I. Romieu, R. Room, L. C. Rosenfeld, A. Roy, L. Rushton, J. A. Salomon, U. Sampson, L. Sanchez-Riera, E. Sanman, A. Sapkota, S. Seedat, P. Shi, K. Shield, R. Shivakoti, G. M. Singh, D. A. Sleet, E. Smith, K. R. Smith, N. J. Stapelberg, K. Steenland, H. Stöckl, L. J. Stovner, K. Straif, L. Straney, G. D. Thurston, J. H. Tran, R. Van Dingenen, A. Van Donkelaar, J. L. Veerman, L. Vijayakumar, R. Weintraub, M.

M. Weissman, R. A. White, H. Whiteford, S. T. Wiersma, J. D. Wilkinson, H. C. Williams, W. Williams, N. Wilson, A. D. Woolf, P. Yip, J. M. Zielinski, A. D. Lopez, C. J. Murray and M. Ezzati, A comparative risk assessment of burden of disease and injury attributable to 67 risk factors and risk factor clusters in 21 regions, 1990–2010: a systematic analysis for the Global Burden of Disease Study 2010, *The Lancet*, 2012, **380**, 2224-2260.

3. N. Li, T. Xia and A. E. Nel, The role of oxidative stress in ambient particulate matter-induced lung diseases and its implications in the toxicity of engineered nanoparticles, *Free Radical Biology and Medicine*, 2008, **44**, 1689-1699.

4. L. Risom, P. Møller and S. Loft, Oxidative stress-induced DNA damage by particulate air pollution, *Mutation Research/Fundamental and Molecular Mechanisms of Mutagenesis*, 2005, **592**, 119-137.

5. I. Fridovich, Fundamental Aspects of Reactive Oxygen Species, or What's the Matter with Oxygen?, *Annals of the New York Academy of Sciences*, 1999, **893**, 13-18.

6. N. Li, M. Hao, R. F. Phalen, W. C. Hinds and A. E. Nel, Particulate air pollutants and asthma: a paradigm for the role of oxidative stress in PM-induced adverse health effects, *Clin. Immunol.*, 2003, **109**, 250.

7. S. A. Gurgueira, J. Lawrence, B. Coull, G. G. K. Murthy and B. González-Flecha, Rapid increases in the steady-state concentration of reactive oxygen species in the lungs and heart after particulate air pollution inhalation, *Environmental health perspectives*, 2002, **110**, 749-755.

8. F. Tao, B. Gonzalez-Flecha and L. Kobzik, Reactive oxygen species in pulmonary inflammation by ambient particulates, *Free Radical Biology and Medicine*, 2003, **35**, 327-340.

9. L. Castro and B. A. Freeman, Reactive oxygen species in human health and disease, *Nutrition*, 2001, **17**, 161-165.

10. J. R. Krall, G. B. Anderson, F. Dominici, M. L. Bell and R. D. Peng, Short-term Exposure to Particulate Matter Constituents and Mortality in a National Study of U.S. Urban Communities, *Environmental Health Perspectives*, 2013, **121**, 1148-1153.

11. M. A. A. Schoonen, C. A. Cohn, E. Roemer, R. Laffers, S. R. Simon and T. O'Riordan, Mineral-Induced Formation of Reactive Oxygen Species, *Reviews in Mineralogy and Geochemistry*, 2006, **64**, 179-221.

12. S. L. Rees, A. L. Robinson, A. Khlystov, C. O. Stanier and S. N. Pandis, Mass balance closure and the Federal Reference Method for PM2.5 in Pittsburgh, Pennsylvania, *Atmospheric Environment*, 2004, **38**, 3305-3318.

13. J. G. Charrier and C. Anastasio, On dithiothreitol (DTT) as a measure of oxidative potential for ambient particles: evidence for the importance of soluble transition metals, *Atmos. Chem. Phys.*, 2012, **12**, 9321.

14. M. Chevion, A site-specific mechanism for free radical induced biological damage: The essential role of redox-active transition metals, *Free Radical Biology and Medicine*, 1988, **5**, 27-37.

15. B. Frei, Reactive oxygen species and antioxidant vitamins: Mechanisms of action, *The American Journal of Medicine*, 1994, **97**, S5-S13.

16. A. Saffari, N. Daher, M. M. Shafer, J. J. Schauer and C. Sioutas, Global Perspective on the Oxidative Potential of Airborne Particulate Matter: A Synthesis of Research Findings, *Environ. Sci. Technol.*, 2014, **48**, 7576.

17. J. T. Bates, T. Fang, V. Verma, L. Zeng, R. J. Weber, P. E. Tolbert, J. Y. Abrams, S. E. Sarnat, M. Klein, J. A. Mulholland and A. G. Russell, Review of Acellular Assays of Ambient Particulate Matter Oxidative Potential: Methods and Relationships with Composition, Sources, and Health Effects, *Environmental Science & Technology*, 2019, **53**, 4003-4019.

18. S. Dikalov, K. K. Griendling and D. G. Harrison, Measurement of Reactive Oxygen Species in Cardiovascular Studies, *Hypertension*, 2007, **49**, 717-727.

19. A. K. Cho, C. Sioutas, A. H. Miguel, Y. Kumagai, D. A. Schmitz, M. Singh, A. Eiguren-Fernandez and J. R. Froines, Redox Activity of Airborne Particulate Matter at Different Sites in the Los Angeles Basin, *Environ. Res.*, 2005, **99**, 40.

20. Jiang, Ahmed, Canchola, Chen and Lin, Use of Dithiothreitol Assay to Evaluate the Oxidative Potential of Atmospheric Aerosols, *Atmosphere*, 2019, **10**, 571.

21. K. R. Daellenbach, G. Uzu, J. Jiang, L.-E. Cassagnes, Z. Leni, A. Vlachou, G. Stefenelli, F. Canonaco, S. Weber, A. Segers, J. J. P. Kuenen, M. Schaap, O. Favez, A. Albinet, S. Aksoyoglu, J. Dommen, U. Baltensperger, M. Geiser, I. El Haddad, J.-L. Jaffrezo and A. S. H. Prévôt, Sources of particulate-matter air pollution and its oxidative potential in Europe, *Nature*, 2020, **587**, 414-419.

22. T. Fang, L. H. Zeng, D. Gao, V. Verma, A. B. Stefaniak and R. J. Weber, Ambient Size Distributions and Lung Deposition of Aerosol Dithiothreitol-Measured Oxidative Potential: Contrast between Soluble and Insoluble Particles, *Environ. Sci. Technol.*, 2017, **51**, 6802.

23. V. Verma, T. Fang, L. Xu, R. E. Peltier, A. G. Russell, N. L. Ng and R. J. Weber, Organic Aerosols Associated with the Generation of Reactive Oxygen Species (ROS) by Water-Soluble PM2.5, *Environ. Sci. Technol.*, 2015, **49**, 4646.

24. V. Verma, T. Fang, H. Guo, L. King, J. T. Bates, R. E. Peltier, E. Edgerton, A. G. Russell and R. J. Weber, Reactive oxygen species associated with water-soluble PM2.5 in the southeastern United States: spatiotemporal trends and source apportionment, *Atmos. Chem. Phys.*, 2014, **14**, 12915.

25. A. Saffari, S. Hasheminassab, M. M. Shafer, J. J. Schauer, T. A. Chatila and C. Sioutas, Nighttime aqueous-phase secondary organic aerosols in Los Angeles and its implication for fine particulate matter composition and oxidative potential, *Atmos. Environ.*, 2016, **133**, 112.

26. C.-H. Jeong, A. Traub, A. Huang, N. Hilker, J. M. Wang, D. Herod, E. Dabek-Zlotorzynska, V. Celo and G. J. Evans, Long-term analysis of PM2.5 from 2004 to 2017 in Toronto: Composition, sources, and oxidative potential, *Environmental Pollution*, 2020, **263**, 114652.

27. S. Weichenthal, M. Shekarrizfard, A. Traub, R. Kulka, K. Al-Rijleh, S. Anowar, G. Evans and M. Hatzopoulou, Within-City Spatial Variations in Multiple Measures of PM2.5 Oxidative Potential in Toronto, Canada, *Environmental Science & Technology*, 2019, **53**, 2799-2810.

28. X. Li, X. M. Kuang, C. Yan, S. Ma, S. E. Paulson, T. Zhu, Y. Zhang and M. Zheng, Oxidative Potential by PM2.5 in the North China Plain: Generation of Hydroxyl Radical, *Environmental Science & Technology*, 2019, **53**, 512-520.

29. R. W. Atkinson, E. Samoli, A. Analitis, G. W. Fuller, D. C. Green, H. R. Anderson, E. Purdie, C. Durister, L. Aitlhadj, F. J. Kelly and I. S. Mudway, Short-term associations between particle oxidative potential and daily mortality and hospital admissions in London, *Int. J. Hyg. Environ. Health*, 2016, **219**, 566.

30. C. Canova, C. Minelli, C. Dunster, F. Kelly, P. L. Shah, C. Caneja, M. K. Tumilty and P. Burney, PM10 Oxidative Properties and Asthma and COPD, *Epidemiology*, 2014, **25**, 467.

31. Y. Kumagai, S. Koide, K. Taguchi, A. Endo, Y. Nakai, T. Yoshikawa and N. Shimojo, Oxidation of Proximal Protein Sulfhydryls by Phenanthraquinone, a Component of Diesel Exhaust Particles, *Chemical Research in Toxicology*, 2002, **15**, 483-489.

32. T. Fang, V. Verma, H. Guo, L. E. King, E. S. Edgerton and R. J. Weber, A semi-automated system for quantifying the oxidative potential of ambient particles in aqueous extracts using the dithiothreitol (DTT) assay: results from the Southeastern Center for Air Pollution and Epidemiology (SCAPE), *Atmos. Meas. Tech.*, 2015, **8**, 471.

33. Q. Xiong, H. Yu, R. Wang, J. Wei and V. Verma, Rethinking Dithiothreitol-Based Particulate Matter Oxidative Potential: Measuring Dithiothreitol Consumption versus Reactive Oxygen Species Generation, *Environmental Science & Technology*, 2017, **51**, 6507-6514.

34. F. Shirmohammadi, S. Hasheminassab, D. B. Wang, J. J. Schauer, M. M. Shafer, R. J. Delfino and C. Sioutas, The relative importance of tailpipe and non-tailpipe emissions on the oxidative potential of ambient particles in Los Angeles, CA, *Faraday Discuss.*, 2016, **189**, 361.

35. N. Li, C. Sioutas, A. Cho, D. Schmitz, C. Misra, J. Sempf, M. Wang, T. Oberley, J. Froines and A. Nel, Ultrafine particulate pollutants induce oxidative stress and mitochondrial damage, *Environmental Health Perspectives*, 2003, **111**, 455-460.

36. B. E. Reed, J. Yalamanchili, J. B. Leach and C. J. Hennigan, Fate of transition metals in PO4-based in vitro assays: equilibrium modeling and macroscopic studies, *Environmental Science: Processes & Impacts*, 2021.

37. C. M. H. Ferreira, I. S. S. Pinto, E. V. Soares and H. M. V. M. Soares, (Un)suitability of the use of pH buffers in biological, biochemical and environmental studies and their interaction with metal ions – a review, *RSC Advances*, 2015, **5**, 30989-31003.

38. M. Ghanem, E. Perdrix, L. Y. Alleman, D. Rousset and P. Coddeville, Phosphate Buffer Solubility and Oxidative Potential of Single Metals or Multielement Particles of Welding Fumes, *Atmosphere*, 2020, **12**, 30.

39. C. Connell, *Phosphorus removal and disposal from municipal wastewater*, Environmental Protection Agency, Office of Research and Monitoring, Washington, D.C. , 1971.

40. C. Ratanatamskul, C. Chiemchaisri and K. Yamamoto, The use of a zeolite-iron column for residual ammonia and phosphorus removal in the effluent from a membrane process as an on-site small-scale domestic wastewater treatment, *Water Science and Technology*, 1995, **31**, 145-152.

41. R.-h. Li, J.-l. Cui, X.-d. Li and X.-y. Li, Phosphorus Removal and Recovery from Wastewater using Fe-Dosing Bioreactor and Cofermentation: Investigation by X-ray Absorption Near-Edge Structure Spectroscopy, *Environmental Science & Technology*, 2018, **52**, 14119-14128.

42. F. Shirmohammadi, S. Hasheminassab, D. Wang, A. Saffari, J. J. Schauer, M. M. Shafer, R. J. Delfino and C. Sioutas, Oxidative potential of coarse particulate matter (PM10–2.5) and its relation to water solubility and sources of trace elements and metals in the Los Angeles Basin, *Environmental Science: Processes & Impacts*, 2015, **17**, 2110-2121.

43. D. Wang, P. Pakbin, M. M. Shafer, D. Antkiewicz, J. J. Schauer and C. Sioutas, Macrophage reactive oxygen species activity of water-soluble and water-insoluble fractions of ambient coarse, PM2.5 and ultrafine particulate matter (PM) in Los Angeles, *Atmospheric Environment*, 2013, **77**, 301-310.

44. P. S. Nico, B. M. Kumfer, I. M. Kennedy and C. Anastasio, Redox Dynamics of Mixed Metal (Mn, Cr, and Fe) Ultrafine Particles, *Aerosol Science and Technology*, 2009, **43**, 60-70.

45. A. S. Teja and P.-Y. Koh, Synthesis, properties, and applications of magnetic iron oxide nanoparticles, *Progress in Crystal Growth and Characterization of Materials*, 2009, **55**, 22-45.

46. W. Rattanavaraha, E. Rosen, H. F. Zhang, Q. F. Li, K. Pantong and R. M. Kamens, The reactive oxidant potential of different types of aged atmospheric particles: An outdoor chamber study, *Atmos. Environ.*, 2011, **45**, 3848.

47. V. Verma, R. Rico-Martinez, N. Kotra, L. King, J. Liu, T. W. Snell and R. J. Weber, Contribution of Water-Soluble and Insoluble Components and Their Hydrophobic/Hydrophilic Subfractions to the Reactive Oxygen Species-Generating Potential of Fine Ambient Aerosols, *Environmental Science & Technology*, 2012, **46**, 11384-11392.

48. A. Yang, A. Jedynska, B. Hellack, I. Rooter, G. Hoek, B. Brunekreef, T. A. J. Kuhlbusch, F. R. Cassee and N. A. H. Janssen, Measurement of the oxidative potential of PM2.5 and

its constituents: The effect of extraction solvent and filter type, *Atmos. Environ.*, 2014, **83**, 35.

49. E. Vidrio, H. Jung and C. Anastasio, Generation of hydroxyl radicals from dissolved transition metals in surrogate lung fluid solutions, *Atmos. Environ.*, 2008, **42**, 4369.

50. C. J. Hennigan, A. Mucci and B. E. Reed, Trends in PM 2.5 transition metals in urban areas across the United States, *Environmental Research Letters*, 2019, **14**, 104006.

51. Y. Fujitani, A. Furuyama, K. Tanabe and S. Hirano, Comparison of Oxidative Abilities of PM2.5 Collected at Traffic and Residential Sites in Japan. Contribution of Transition Metals and Primary and Secondary Aerosols, *Aerosol Air Qual. Res.*, 2017, **17**, 574.

52. M. Lin and J. Z. Yu, Dithiothreitol (DTT) concentration effect and its implications on the applicability of DTT assay to evaluate the oxidative potential of atmospheric aerosol samples, *Environmental Pollution*, 2019, **251**, 938-944.

53. H. A. Bamford, D. Z. Bezabeh, M. M. Schantz, S. A. Wise and J. E. Baker, Determination and comparison of nitrated-polycyclic aromatic hydrocarbons measured in air and diesel particulate reference materials, *Chemosphere*, 2003, **50**, 575-587.

54. Y. Wang and M. Tang, PM2.5 induces ferroptosis in human endothelial cells through iron overload and redox imbalance, *Environmental Pollution*, 2019, **254**, 112937.

55. Y. Wang and M. Tang, PM2.5 induces autophagy and apoptosis through endoplasmic reticulum stress in human endothelial cells, *Science of The Total Environment*, 2020, **710**, 136397.

56. Y. Wang, L. Xiong, L. Zou, Y. Liang, W. Xie, Y. Ma, X. Huang and M. Tang, Subacute episodic exposure to environmental levels of atmospheric particulate matter provokes subcellular disequilibrium instead of histological vascular damage, *Journal of Hazardous Materials Letters*, 2021, **2**, 100045.

57. T. Wang, L. Wang, S. R. Zaidi, S. Sammani, J. Siegler, L. Moreno-Vinasco, B. Mathew, V. Natarajan and J. G. N. Garcia, Hydrogen Sulfide Attenuates Particulate Matter–Induced Human Lung Endothelial Barrier Disruption via Combined Reactive Oxygen Species Scavenging and Akt Activation, *American Journal of Respiratory Cell and Molecular Biology*, 2012, **47**, 491-496.

58. P. Maciejczyk, L.-C. Chen and G. Thurston, The Role of Fossil Fuel Combustion Metals in PM2.5 Air Pollution Health Associations, *Atmosphere*, 2021, **12**, 1086.

59. P. E. Pfeffer, H. Lu, E. H. Mann, Y.-H. Chen, T.-R. Ho, D. J. Cousins, C. Corrigan, F. J. Kelly, I. S. Mudway and C. M. Hawrylowicz, Effects of vitamin D on inflammatory and oxidative stress responses of human bronchial epithelial cells exposed to particulate matter, *PLOS ONE*, 2018, **13**, e0200040.

60. A. Gawda, G. Majka, B. Nowak, M. Śróttek, M. Walczewska and J. Marcinkiewicz, Air particulate matter SRM 1648a primes macrophages to hyperinflammatory response after LPS stimulation, *Inflammation Research*, 2018, **67**, 765-776.

61. O. Mazuryk, G. Stochel and M. Brindell, Variations in Reactive Oxygen Species Generation by Urban Airborne Particulate Matter in Lung Epithelial Cells-Impact of Inorganic Fraction, *Frontiers in chemistry*, 2020, **8**, 581752-581752.

62. M. Mikrut, O. Mazuryk, W. Macyk, R. van Eldik and G. Stochel, Generation and photogeneration of hydroxyl radicals and singlet oxygen by particulate matter and its inorganic components, *Journal of Environmental Chemical Engineering*, 2021, **9**, 106478.

63. D. Salcedo, B. J.P, O. Erez-Arvizu and E. Lounejeva, Assessment of sample preparation methods for the analysis of trace elements in airborne particulate matter, *Journal of Analytical Atomic Spectrometry*, 2014, **29**.

64. A. Albinet, G. M. Lanzafame, D. Srivastava, N. Bonnaire, F. Nalin and S. A. Wise, Analysis and determination of secondary organic aerosol (SOA) tracers (markers) in particulate matter standard reference material (SRM 1649b, urban dust), *Analytical and Bioanalytical Chemistry*, 2019, **411**, 5975-5983.

65. E. Conca, M. Malandrino, A. Giacomino, E. Costa, F. Ardini, P. Inaudi and O. Abollino, Optimization of a sequential extraction procedure for trace elements in Arctic PM10, *Analytical and Bioanalytical Chemistry*, 2020, **412**, 7429-7440.

66. R. J. Mitkus, J. L. Powell, R. Zeisler and K. S. Squibb, Comparative physicochemical and biological characterization of NIST Interim Reference Material PM2.5 and SRM 1648 in human A549 and mouse RAW264.7 cells, *Toxicology in Vitro*, 2013, **27**, 2289-2298.

67. L. Hendriks, B. Ramkorun-Schmidt, A. Gundlach-Graham, J. Koch, R. N. Grass, N. Jakubowski and D. Günther, Single-particle ICP-MS with online microdroplet calibration: toward matrix independent nanoparticle sizing, *Journal of Analytical Atomic Spectrometry*, 2019, **34**, 716-728.

68. E. McCurdy and W. Proper, Improving ICP-MS Analysis of Samples Containing High Levels of Total Dissolved Solids, *Spectroscopy*, 2014, **29**, 14.

69. A. K. Cho, C. Sioutas, A. H. Miguel, Y. Kumagai, D. A. Schmitz, M. Singh, A. Eiguren-Fernandez and J. R. Froines, Redox activity of airborne particulate matter at different sites in the Los Angeles Basin, *Environ. Res.*, 2005, **99**, 40.

70. D. F. Driscoll, F. Etzler, T. A. Barber, J. Nehne, W. Niemann and B. R. Bistrian, Physicochemical assessments of parenteral lipid emulsions: light obscuration versus laser diffraction, *International Journal of Pharmaceutics*, 2001, **219**, 21-37.

71. A. Kumar, V. Subramanian, S. K. Velaga, J. Kodandaraman, P. N. Sujatha, R. Baskaran, S. Kumar and B. M. Ananda Rao, Performance evaluation of a tubular bowl centrifuge by using laser obscuration method as an online measurement tool, *Separation Science and Technology*, 2020, **55**, 1839-1851.

72. F. Storti and F. Balsamo, Particle size distributions by laser diffraction: sensitivity of granular matter strength to analytical operating procedures, *Solid Earth*, 2010, **1**, 25-48.

73. Q. Liu, Z. Tang, Z. Zhou, H. Zhou, B. Ou, B. Liao, S. Shen and L. Chen, A Novel Route to Prepare Cationic Polystyrene Latex Particles with Monodispersity, *Journal of Macromolecular Science, Part A*, 2014, **51**, 271-278.

74. A. Beekman, D. Shan, A. Ali, W. Dai, S. Ward-Smith and M. Goldenberg, Micrometer-Scale Particle Sizing by Laser Diffraction: Critical Impact of the Imaginary Component of Refractive Index, *Pharmaceutical Research*, 2005, **22**, 518-522.

75. M. Li, W. Zhu and L. Gao, Analysis of Cell Concentration, Volume Concentration, and Colony Size of Microcystis Via Laser Particle Analyzer, *Environmental Management*, 2014, **53**, 947-958.

76. E. V. Uspenskaya, T. V. Pleteneva, I. V. Kazimova and A. V. Syroeshkin, Evaluation of Poorly Soluble Drugs' Dissolution Rate by Laser Scattering in Different Water Isotopologues, *Molecules*, 2021, **26**, 601.

77. M. Chang, M. W. McBroom and R. Scott Beasley, Roofing as a source of nonpoint water pollution, *Journal of Environmental Management*, 2004, **73**, 307-315.

78. H. T. Q. Kieu, E. Müller and H. Horn, Heavy metal removal in anaerobic semi-continuous stirred tank reactors by a consortium of sulfate-reducing bacteria, *Water Research*, 2011, **45**, 3863-3870.

79. J. A. Franz, R. J. Williams, J. R. V. Flora, M. E. Meadows and W. G. Irwin, Electrolytic oxygen generation for subsurface delivery: effects of precipitation at the cathode and an assessment of side reactions, *Water Research*, 2002, **36**, 2243-2254.

80. HACH DR 890 Portable colorimeter website, https://www.hach.com/dr-890-portable-colorimeter/product-downloads?id=7640439041).

81. MINEQL equilibrium software website, https://mineql.com/).

82. M. P. Tolocka, P. A. Solomon, W. Mitchell, G. A. Norris, D. B. Gemmill, R. W. Wiener, R. W. Vanderpool, J. B. Homolya and J. Rice, East versus West in the US: Chemical Characteristics of PM2.5during the Winter of 1999, *Aerosol Science and Technology*, 2001, **34**, 88-96.

83. E. DiStefano, A. Eiguren-Fernandez, R. J. Delfino, C. Sioutas, J. R. Froines and A. K. Cho, Determination of metal-based hydroxyl radical generating capacity of ambient and diesel exhaust particles, *Inhalation Toxicol.*, 2009, **21**, 731.

84. Y. Lyu, H. Guo, T. Cheng and X. Li, Particle Size Distributions of Oxidative Potential of Lung-Deposited Particles: Assessing Contributions from Quinones and Water-Soluble Metals, *Environmental Science & Technology*, 2018, **52**, 6592-6600.

85. J. G. Charrier and C. Anastasio, Impacts of antioxidants on hydroxyl radical production from individual and mixed transition metals in a surrogate lung fluid, *Atmos. Environ.*, 2011, **45**, 7555.

86. R. Kohen and A. Nyska, Invited Review: Oxidation of Biological Systems: Oxidative Stress Phenomena, Antioxidants, Redox Reactions, and Methods for Their Quantification, *Toxicologic Pathology*, 2002, **30**, 620-650.

87. M. Lin and J. Z. Yu, Effect of metal-organic interactions on the oxidative potential of mixtures of atmospheric humic-like substances and copper/manganese as investigated by the dithiothreitol assay, *Science of The Total Environment*, 2019, **697**, 134012.

88. J. Wei, H. Yu, Y. Wang and V. Verma, Complexation of Iron and Copper in Ambient Particulate Matter and Its Effect on the Oxidative Potential Measured in a Surrogate Lung Fluid, *Environmental Science & Technology*, 2019, **53**, 1661-1671.

89. V. Verma, Z. Ning, A. K. Cho, J. J. Schauer, M. M. Shafer and C. Sioutas, Redox activity of urban quasi-ultrafine particles from primary and secondary sources, *Atmos. Environ.*, 2009, **43**, 6360.

90. G. Karavalakis, N. Gysel, D. A. Schmitz, A. K. Cho, C. Sioutas, J. J. Schauer, D. R. Cocker and T. D. Durbin, Impact of biodiesel on regulated and unregulated emissions, and redox and proinflammatory properties of PM emitted from heavy-duty vehicles, *Science of The Total Environment*, 2017, **584-585**, 1230-1238.

91. M. R. C. Marques, R. Loebenberg and M. Almukainzi, Simulated Biological Fluids with Possible Application in Dissolution Testing, *Dissolution Technologies*, 2011, **18**, 15-28.